Water Research 232 (2023) 119663

Contents lists available at ScienceDirect

Water Research

journal homepage: www.elsevier.com/locate/watres

# Geochemistry, stable isotopes and statistic tools to estimate threshold and source of nitrate in groundwater (Sardinia, Italy)

Riccardo Biddau [a], Elisabetta Dore [a,*], Stefania Da Pelo [a], Mario Lorrai [b], Paolo Botti [b], Maurizio Testa [c], Rosa Cidu [a]

[a] Department of Chemical and Geological Sciences, University of Cagliari, Blocco A - Monserrato, Italy
[b] Regione Autonoma della Sardegna-ADIS-Servizio tutela e gestione delle risorse idriche, via Mameli 88, 09100, Cagliari, Italy
[c] Agenzia Regionale per la Protezione dell'Ambiente della Sardegna - Servizio Controlli, Monitoraggi e Valutazione Ambientale della Direzione Tecnico Scientifica, via Carloforte, 09100, Cagliari, Italy

ARTICLE INFO

*Keywords:*
Groundwater
Nitrate pollution
Stable isotopes
Mixing models
Sardinia

ABSTRACT

In the European Union, nitrate vulnerable zone (NVZ) should be designed for the mitigation of nitrate ($NO_3^-$) contamination caused by agricultural practices. Before establishing new NVZ, the sources of $NO_3^-$ must be recognized. A geochemical and multiple stable isotopes approach (hydrogen, oxygen, nitrogen, sulfur and boron) and statistical tools were applied to define the geochemical characteristics of groundwater (60 samples), calculate the local $NO_3^-$ threshold and assess potential sources of $NO_3^-$ contamination in two study areas (hereafter Northern and Southern), located in a Mediterranean environment (Sardinia, Italy). Results of the integrated approach applied to two case study, permits to highlight the strengths of integrating geochemical and statistical methods to provide nitrate source identification as a reference by decision makers to remediate and mitigate nitrate contamination in groundwater.

Hydrogeochemical features in the two study areas were similar: near neutral to slightly alkaline pH, electrical conductivity in the range of 0.3 to 3.9 mS/cm, and chemical composition ranging from Ca-$HCO_3^-$ at low salinity to Na-$Cl^-$ at high salinity. Concentrations of $NO_3^-$ in groundwater were in the range of 1 to 165 mg/L, whereas the nitrogen reduced species were negligible, except few samples having $NH_4^+$ up to 2 mg/L. Threshold values in the studied groundwater samples were between 4.3 and 6.6 mg/L $NO_3^-$, which was in agreement with previous estimates in Sardinian groundwater.

Values of $\delta^{34}S$ and $\delta^{18}O_{SO4}$ of $SO_4^{2-}$ in groundwater samples indicated different sources of $SO_4^{2-}$. Sulfur isotopic features attributed to marine $SO_4^{2-}$ were consistent with groundwater circulation in marine-derived sediments. Other source of $SO_4^{2-}$ were recognize due to the oxidation of sulfide minerals, to fertilizers, manure, sewage fields, and $SO_4^{2-}$ derived from a mix of different sources.

Values of $\delta^{15}N$ and $\delta^{18}O_{NO3}$ of $NO_3^-$ in groundwater samples indicated different biogeochemical processes and $NO_3^-$ sources. Nitrification and volatilization processes might have occurred at very few sites, and denitrification was likely to occur at specific sites. Mixing among various $NO_3^-$ sources in different proportions might account for the observed $NO_3^-$ concentrations and the nitrogen isotopic compositions. The SIAR modeling results showed a prevalent $NO_3^-$ source from sewage/manure. The $\delta^{11}B$ signatures in groundwater indicated the manure to be the predominant $NO_3^-$ source, whereas $NO_3^-$ from sewage was recognized at few sites. Geographic areas showing either a predominant process or a defined $NO_3^-$ source where not recognize in the studied groundwater. Results indicate widespread contamination of $NO_3^-$ in the cultivated plain of both areas. Point sources of contamination, due to agricultural practices and/or inadequate management of livestock and urban wastes, were likely to occur at specific sites.

* Corresponding author.
*E-mail address:* elisabetta.dore@unica.it (E. Dore).

https://doi.org/10.1016/j.watres.2023.119663
Received 10 August 2022; Received in revised form 15 December 2022; Accepted 22 January 2023
Available online 24 January 2023

## 1. Introduction

Large amounts of water resources of the world are affected by nitrate pollution that negatively impacts on human health and ecosystems. Natural waters may contain different nitrogen species, i.e. dissolved gas from the atmosphere ($N_2$), ammonia ($NH_3$) from rain and soil, the ions ammonium ($NH_4^+$), nitrite ($NO_2^-$) and nitrate ($NO_3^-$), and organic nitrogen compounds (Stumm and Morgan, 1996). Sources of nitrogen ions include the soil, fertilizers, sewage, manure, industrial effluents, and geologic materials containing soluble nitrogen compounds. Nitrate is the end product of nitrification processes, and is usually taken up by plants. The excess $NO_3^-$ goes into water systems because it is poorly absorbed by clay minerals and is stable in aqueous media unless denitrification processes occur. The $NO_3^-$ stability in solution under a wide range of pH and redox conditions, may result in concentrations above the guideline of 50 mg/L established by the World Health organization (WHO, 2011), which are frequently observed in water systems, including drinking water (Sarkar et al., 2021; Picetti et al., 2022).

Since the 1991, the European Commission has promoted specific measures aimed to minimize $NO_3^-$ contamination derived from agricultural practices (Nitrate Directive – EEC, 1991). Nevertheless, data collected until the 2019 in the European State Members showed that 14.1% of groundwater stations still exceeded 50 mg/L $NO_3^-$ in annual average and that there has been no overall decrease of $NO_3^-$ concentration in groundwater in the last 20 years (EC, 2021). This suggests that further measures should be taken to mitigate groundwater contamination by $NO_3^-$. Before establishing new rules for contaminated areas, the sources of $NO_3^-$ must be recognized.

Different approaches have been used to track $NO_3^-$ sources in groundwater: the water chemistry, isotopic signatures, microbial composition, statistics, and combinations of them (Menció et al., 2016; Kazakis et al., 2020; Cao et al., 2022). In particular, due to the peculiar isotopic signatures of different sources, multiple stable isotopes (Martinelli et al., 2018; Yu et al., 2020; Carrey et al., 2021; Ryu et al., 2021; He et al., 2022) and statistical models (i.e.: Bayesian SIAR model, Parnell et al., 2013; Meghdadi and Javar, 2018; Ren et al., 2022) has been used to quantify the relative contributions of potential $NO_3^-$ sources.

In Sardinia (Italy), the intensive dairy cattle district of Arborea has been declared a nitrate vulnerable zone (NVZ) in 2005, and a specific action program for the reduction of $NO_3^-$ has been developed (RAS, 2005; ARPAS, 2009; Biddau et al., 2019). However, other wells in Sardinia (than those located within the Arborea NVZ) showed $NO_3^-$ concentrations above 50 mg/L that persisted several years, thus demanding targeted actions to reduce the contamination. According to the Groundwater Directive and the Nitrate Directive (EEC, 1991; EC, 2006), the European Member States are required to identify groundwater bodies (GWBs) at risk of failing to meet the environmental objectives, as well to designate as NVZ the areas being at risk from agricultural nitrate pollution. This study was aimed at investigating two areas to be eventually designated as new NVZ in Sardinia. To this purpose it presents a preliminary evaluation of the effectiveness of the more widely used approaches targeted to the identification of nitrate contamination origin when multiple inputs are present. Specific objectives were to: *i)* define the geochemical characteristics of groundwater samples; *ii)* calculate the local threshold of $NO_3^-$ in groundwater; *iii)* investigate the behavior of deuterium, oxygen-18, nitrogen-15, sulfur-34 and boron-11 stable isotopes to recognize the potential sources of nitrate contamination.

## 2. Study areas

The areas selected for this investigation are located in the North and South Sardinia (Fig. 1). Climate is Mediterranean with warm dry summers and mild rainy winters. The mean annual temperature is 15.9 °C and mean annual precipitation is 537 mm, the latter mostly concentrated between October and March (Frau et al., 2020). Land uses consist of woodland, Mediterranean maquis, orchards, olive groves, arable fields and natural grazing; greenhouses are mostly located in the South (RAS, 2013a).

Main geological features of Sardinia consist of a segment of the western European Variscan metamorphic basement, covered by continental Upper Carboniferous–Permian sedimentary and volcanic deposits, Mesozoic carbonatic shelf sediments, Tertiary to Quaternary volcanic and sedimentary sequences (Sinisi et al., 2012).

Geological features in the Northern zone are comprised of shallow marine sediments with evaporite and carbonate (Middle Triassic to Middle Cretaceous), volcanic rocks ranging from basaltic to rhyolitic in composition (Sinisi et al., 2012) and sedimentary Miocene sequences made up of marl sandstone, siltstone, limestone and conglomerate (Upper Burdigalian-Tortonian, Funedda et al., 2000).

The Southern zone is located in the southernmost portion of the Campidano Graben (Middle Pliocene, Cocco et al., 2012, 2013), filled up by sand, mud, conglomerate, lacustrine clay and, more recently, by fluvial deposits (Angelone et al., 2005, and references therein). A relevant industrial area (about 9000 ha) is included in the Southern area, which includes chemical and petro-chemical plants, port activities, refineries and incinerators (Frontalini et al., 2009).

According to the requirements of the European Water Framework Directive (EC, 2000), thirty-eight main hydrogeologic complexes were recognized in Sardinia. They are constituted of one or more hydrogeologic units, with homogenous lithology and degree of permeability and are divided in 114 GWBs. The investigated GWBs are hosted in Pliocene-Quaternary sediments (CIS 0511, 0121, 1721, 1722), in Oligocene-Miocene detritus-carbonatic sediments (CIS 2311, 2312, 2321) and in Mesozoic carbonatic rocks (CIS 3211), with locations and main groundwater flow directions shown in Fig. 1.

## 3. Sampling and methods

Samples for this study were collected in the framework of the groundwater monitoring program established by the Sardinian Region. This program is a long-term activity aimed to identify temporal trends in groundwater quality at the regional scale. Monitoring stations include fresh groundwater from relevant aquifers, drinking water supply sites, groundwater in areas of environmental relevance (e.g.: wetlands), and target areas submitted at relevant anthropogenic pressure such as industrial sites. Whiting the monitoring plan, major ions ($Ca^{2+}$, $Mg^{2+}$, $Na^+$, $K^+$, $Cl^-$, $HCO_3^-$, $SO_4^{2-}$, $F^-$, $Br^-$, $PO_4^{3-}$), nitrogen species ($NO_3^-$, $NO_2^-$, $NH_4^+$) and selected trace elements are routinely analyzed twice a year at each monitoring stations and chemical data have been available from 2011.

The monitoring network in the studied areas consists of 112 stations, 48 located in the Northern zone (10 springs and 38 wells) and 64 (wells) in the Southern zone. The location of monitoring stations in the studied areas is shown in Fig. 1. In the studied areas, all monitoring stations were sampled and analyzed whiting the monitoring program in 2018. Nitrate concentrations measured at each station were considered in this study in order to evaluate the spatial distribution of nitrate and estimate the threshold values in both areas. Concentrations of nitrate measured in 2018 were also compared with the average values of nitrate calculated over seven years of monitoring (from 2011 to 2017). During the 2018 survey, B and isotopic analyses ($\delta^2H$ and $\delta^{18}O$ of water, $\delta^{15}N$ and $\delta^{18}O$ of dissolved $NO_3^-$, $\delta^{34}S$ and $\delta^{18}O$ of dissolved $SO_4^{2-}$ and $\delta^{11}B$) were performed at selected stations (29 located in the Northern zone and 31 in the Southern zone) in order to evaluate potential sources of nitrate in the studied areas. The selection of stations was based on: *i)* average concentration of nitrate from previous surveys (were selected both samples with nitrate $>$ 20 mg/L and stations potentially unpolluted with nitrate $<$ 5 mg/L); *ii)* location of monitoring station (were selected stations potentially affected by single and/or multiple sources of nitrate); *iii)* spatial distribution of stations in order to achieve a representative coverage over the studied areas. Data from selected stations, for which the complete dataset (chemistry and isotopes) is available, are discussed

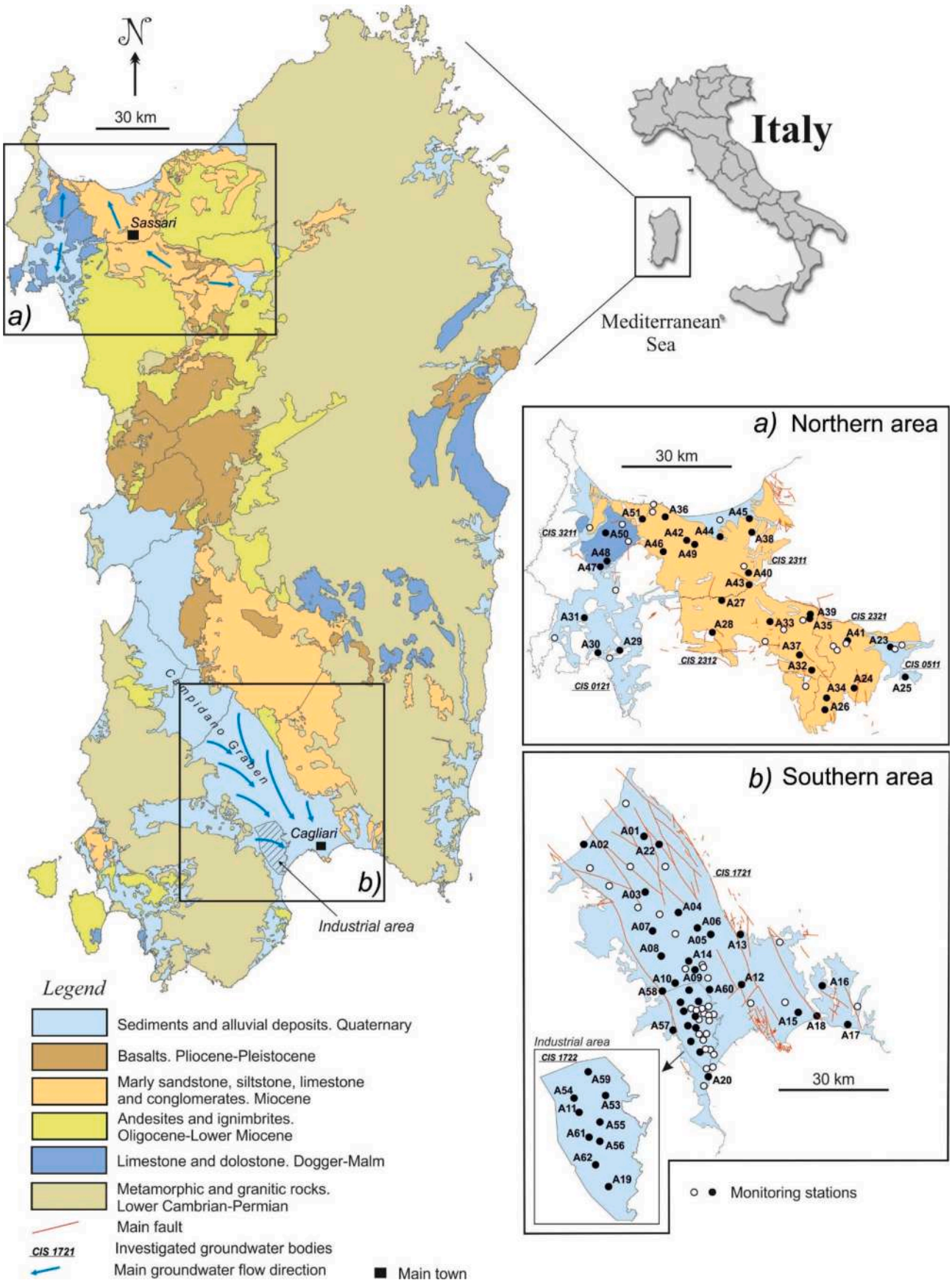


**Fig. 1.** Schematic geology of Sardinia (modified by RAS, 2013b), location of study areas, groundwater bodies (CIS) and location of monitoring stations (black circle refers to the location of selected station for isotopic analyses).

in this study.

In order to characterize the potential source of contamination, 10 samples were collected at urban wastewater treatment plants, which inputs comprised a mix of sewage and run-off rainwater in variable proportions according with seasonality.

In situ, the water table level of wells, flow of springs, temperature, pH, electrical conductivity (EC) and dissolved oxygen were measured. Each well was purged before the collection of water. Immediately upon collection, the water was filtered through 0.22 μm pore-size filters in pre-cleaned high-density PE bottles and keep cooled by a portable refrigerator. One aliquot was acidified with 1% (v/v) $HNO_3$ supra pure, immediately upon filtration, for metal analyses. Aliquots for the nitrate isotope analyses were frozen in situ in order to prevent any alteration due to biological processes.

Analysis of major ions, nitrogen species and Mn were carried out within the framework of the R.A.S. groundwater-monitoring program at certified laboratories (RAS, 2011). Boron and Si were determined at the University of Cagliari by inductively coupled plasma mass spectrometry (ICP-MS) and inductively coupled plasma optical emission spectrometry (ICP-OES). For each analytical run, the detection limits (DL) were calculated at 5 times the standard deviation (SD) plus the mean value calculated on several analyses of the blank solution. The standard reference solutions SRM1643d,e (supplied by the US National Institute of Standard & Technology, Gaithersburg, Maryland) and EnviroMAT ES-L-3 (supplied by SCP Science, St. Laurent, Quebec) were used to estimate analytical errors, which were usually below 5%.

The $\delta^2H$ and $\delta^{18}O_{H2O}$ were measured using Wavelength-Scanned Cavity Ringdown Spectroscopy (L2120-i, Picarro). The $\delta^{15}N$ and $\delta^{18}O_{NO3}$ of $NO_3^-$ were determined by isotope ratio mass spectrometer (IRMS, Finnigan MAT-253, Thermo Scientific). The $\delta^{34}S$ and $\delta^{18}O_{SO4}$ of $SO_4^{2-}$ were determined by IRMS (Carlo Erba EA - Finnigan Delta C - ThermoQuest). Isotopic analyses of water, nitrate and sulfate were performed at the laboratory of the Mineralogia Aplicada i Medi Ambient, University of Barcelona, Spain, with details on analytical methods being reported in Puig et al. (2017). The $\delta^{11}B$ was determined by multi collector sector field ICP-MS (MC-ICP-SFMS) at the Scandinavia ALS Laboratory Group, Sweden, with details on analytical methods being reported in Venturi et al. (2015). Isotopic results were expressed in terms of δ (Coplen, 2011) relative to the international standard Vienna Standard Mean Oceanic Water (V-SMOW) for $\delta^2H$, $\delta^{18}O_{H2O}$, $\delta^{18}O_{NO3}$ and $\delta^{18}O_{SO4}$; the Vienna Canyon Diablo Troilite (V-CDT) for $\delta^{34}S$; the air for $\delta^{15}N$; and NBS951 for $\delta^{11}B$. Analytical errors calculated using international and internal laboratory standards were (±δ‰): 1 $\delta^2H$, 0.15 $\delta^{18}O_{H2O}$, 1.0 $\delta^{18}O_{NO3}$, 0.5 $\delta^{18}O_{SO4}$, 0.6 $\delta^{15}N$, 0.2 $\delta^{34}S$ and 0.05 $\delta^{11}B$.

The nitrate concentrations were fitted with a normal (Gaussian) mixture model (McLachlan and Peel, 2000) to recognize subgroups in the population of waters using the "MIXTOOLS" package (Benaglia et al., 2009) implemented in the R software, a free language for statistical computing (R Development Core Team, 2013). The maximum likelihood estimates of the parameters (mean and standard deviation, SD) with normal distributions for each subgroup was calculated using the expectation maximization (EM) algorithm (Dempster et al., 1977). The mean+2SD values of the population having the lowest $NO_3^-$ concentrations was considered as the threshold value for nitrate in the studied areas. This value was referred as "present-day background" and may include, in addition to naturally derived $NO_3$, soil organic matter from the residue of fertilized and unfertilized crops, products of combustion, evaporation of ammonia ($NH_3$) from synthetic and organic N fertilizer and livestock waste (Panno et al., 2006). The samples with nitrate concentrations above the calculated present-day background would be derived prevalently from human-related sources (synthetic N fertilizers, livestock waste, and septic effluent).

Nitrate produced by nitrification typically has a comparatively low $\delta^{18}O$ relative to atmospheric and fertilizer $NO_3^-$, which is assumed to derive from the fractional contribution of oxygen atoms originating from $O_2$ and water during the biological oxidation of $NH_4^+$ to $NO_3^-$, according to the following experimental equation (Andersson and Hooper, 1983):

$$\delta^{18}O_{NO_3} = 2/3\ \delta^{18}O_{H_2O} + 1/3\ \delta^{18}O_{O_2} \quad (1)$$

where $\delta^{18}O_{H2O}$ represents the measured value in the local groundwater samples and $\delta^{18}O_{O2}$ is the +23.5‰ value for atmospheric $O_2$ (Aravena and Mayer, 2010).

The relative contribution of the potential nitrate sources in groundwater samples were calculated using the Bayesian isotope mixing model in the SIAR package (Stable Isotope Analysis in R, Parnell et al., 2008). Dual-isotopic nitrate values ($\delta^{15}N$ and $\delta^{18}O$ of $NO_3^-$) and five potential local sources: $NH_4$ synthetic fertilizers ($NH_4$-fert.), $NO_3^-$ fertilizers ($NO_3$-fert.), soil organic nitrogen (N-soil), sewage and manure (S-M) were included in the model. The isotopic compositions of selected end-members were assumed from the literature (Torres-Martinez et al., 2021) as follows: $NH_4$-fert.: $\delta^{15}N_{NO3}$ 1.24 ± 1.44‰, $\delta^{18}O_{NO3}$ 3.44 ± 2.47‰; $NO_3$-fert.: $\delta^{15}N_{NO3}$ −0.07 ± 2.85‰, $\delta^{18}O_{NO3}$ 24.12 ± 3.17‰; N-soil: $\delta^{15}N_{NO3}$ 3.26 ± 1.99‰, $\delta^{18}O_{NO3}$ 3.34 ± 2.04‰ and M-S: $\delta^{15}N_{NO3}$: 10.14 ± 4.53‰, $\delta^{18}O_{NO3}$ 5.69 ± 2.91‰.

Geochemical maps were drawn using ArcGIS 10.2 (ESRI, 2013).

## 4. Results and discussion

Physical-chemical features and isotopic data of selected groundwater sampled in the Northern and Southern areas are reported in the Supplementary Material (SM) Table 1 and SM Table 2, respectively.

Concentrations of nitrate measured in selected groundwater during 2018 compared with mean and standard deviation (SD) values of nitrate, calculated over seven years of monitoring (from 2011 to 2017), are reported in SM Table 3.

### 4.1. Nitrate distribution and threshold

Fig. 2 shows the spatial distribution of $NO_3^-$ concentrations in all the monitoring station within the two areas, together with a simplified land use map (modified after RAS, 2013b). Nitrate concentration showed a large variation in the studied areas, from 0.8 to about 100 mg/L (maximum value of 165 mg/L was measured in the northern area) and similar median values (about 30 mg/L $NO_3^-$). In both areas, groundwater samples with relatively low and high $NO_3^-$ concentrations were observed at the same locations, suggesting a probably point sources contamination of $NO_3^-$.

Fig. 3 shows the statistical distribution of log-transformed $NO_3^-$ concentrations for the Northern area (Fig. 3a) and Southern area (Fig. 3b). For each area, the $NO_3^-$ threshold was calculated by the mean+2SD of the population showing the lower concentrations. The resulting threshold values were 6.6 and 4.3 mg/L $NO_3^-$ in groundwater of the Northern and Southern area, respectively. These threshold values were in agreement with the $NO_3^-$ threshold calculated for Sardinian groundwater hosted in granitic and metamorphic rocks (Biddau et al., 2017), and similar to present-day background values reported elsewhere (Kim et al., 2015; Carrey et al., 2021; Sarkar et al., 2021; Manu et al., 2022).

### 4.2. Hydrogeochemistry

In the Northern area the temperature of groundwater ranged from 11 to 22 °C, with median value of 16 °C. The pH was near neutral to slightly alkaline (6.7 - 8.0). Values of EC and dissolved oxygen showed a large range, respectively from 0.7 to 4.0 μS/cm and from 3 to 9 mg/L (SM Table 1). The low salinity waters generally showed calcium-bicarbonate predominant composition, which was consistent with circulation of these waters in Tertiary and Mesozoic carbonate aquifers. At high salinity sodium-chloride composition prevailed, whereas magnesium and sulfate were relatively less abundant. Groundwater samples A35, A37, A41 showed predominant Na-bicarbonate composition (SM

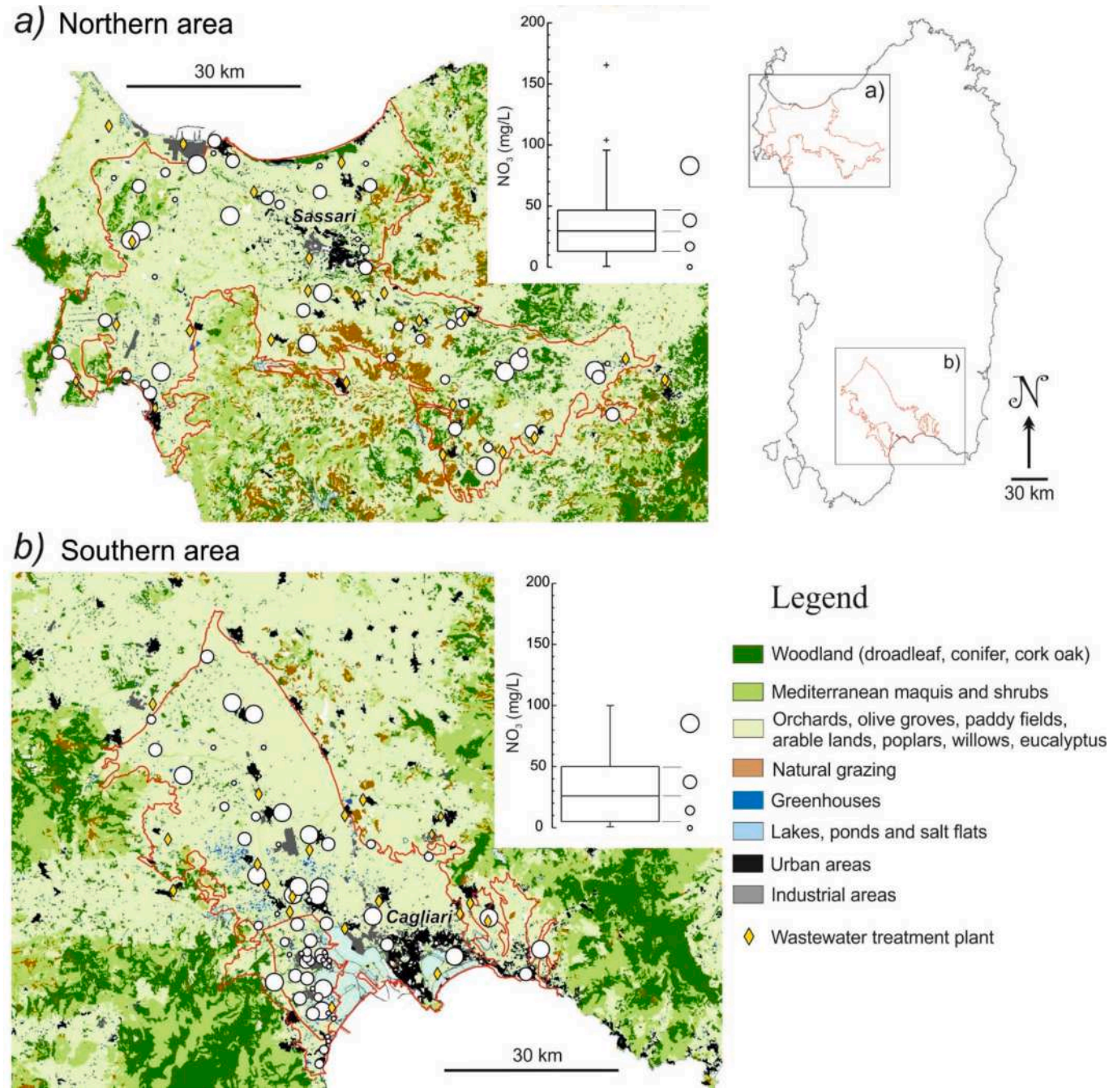


**Fig. 2.** Spatial distribution of $NO_3^-$ concentrations in groundwater from the Northern (a) and Southern (b) areas, superimposed on the simplified soil use map (modified after RAS, 2013a) and boxplot of the $NO_3^-$ concentrations.

Fig. 1a). Concentrations of Na and $Cl^-$ in groundwater followed the seawater dilution line, but few samples were slightly enriched in Na with respect to $Cl^-$, with Na likely derived from the weathering of Na-bearing feldspar. Concentrations of $F^-$ were in the range of 0.05 to 0.8 mg/L (median 0.14 mg/L). Concentrations of $Br^-$ were correlated with $Cl^-$ ($R^2 = 0.941$). The $NO_3^-$ concentrations were in the range of 4 to 165 mg/L, with the highest value showing the highest K concentration (SM Table 1). Reduced nitrogen species were undetectable in most samples; $NO_2^-$ was only detected in 4 samples (up to 2.3 mg/L), and 3.6 mg/L $NH_4^+$ occurred at the outflow of sewage treatment plant (SM Table 1). Concentrations of $SiO_2$ ranged from 3 to 20 mg/L, median value of 7 mg/L, and were not related to temperature. Concentrations of B varied from 19 to 270 μg/L (median 74 μg/L), with values generally increasing with increasing $Cl^-$ ($R^2 = 0.660$). Concentrations of B were not related to temperature, $F^-$ and $SiO_2$.

In the Southern area the temperature of groundwater ranged from 13 to 24 °C. The pH was slightly acidic to alkaline (6.4 - 8.2). Values of EC and dissolved oxygen showed a large range, respectively from 0.3 to 3.9 μS/cm and from 2 to 9 mg/L (SM Table 2). The low salinity waters generally showed Ca-bicarbonate predominant composition; at high salinity the Na-chloride composition prevailed; magnesium and sulfate were relatively low, with the exception of groundwater sample A61 showing a marked Ca-Mg-sulfate composition (SM Fig. 1b). Groundwater samples A3, A15, A56, A58 showed a predominant Na-bicarbonate composition (SM Fig. 1b). Concentrations of Na and $Cl^-$ in groundwater showed molar ratios similar to seawater, with few samples slightly enriched in Na with respect to $Cl^-$. Concentrations of $Br^-$ were correlated with $Cl^-$ ($R^2 = 0.997$). Concentrations of $F^-$ were in

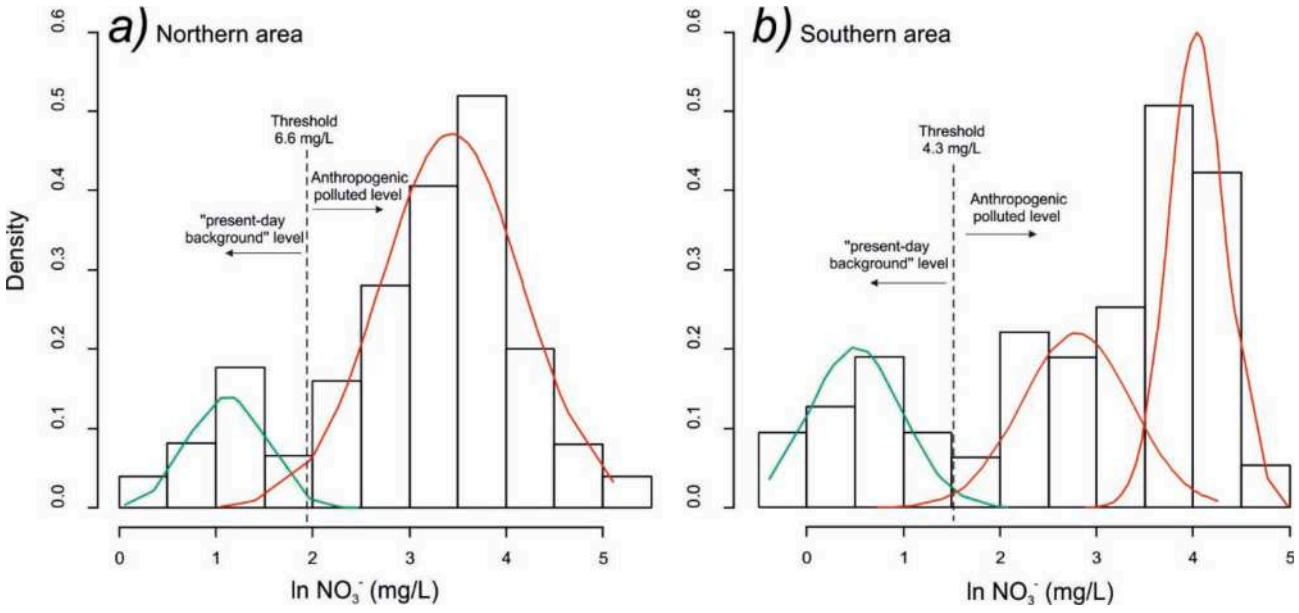


**Fig. 3.** Statistical distributions of log-transformed $NO_3^-$ concentration in groundwater of the Northern (a) and Southern (b) areas, and values of natural $NO_3^-$ threshold estimated on the population having the lowest $NO_3^-$ values (shown in green).

the range of 0.06 to 2.6 mg/L (median 0.17 mg/L). The $NO_3^-$ concentrations were in the range of 1 to 83 mg/L. Reduced nitrogen species were undetectable in most samples, $NO_2^-$ was always < 0.02 mg/L (SM Table 2), and up to 2 mg/L $NH_4^+$ occurred in six samples (SM Table 2). Silica ranged from 2 to 34 mg/L (SM Table 2), with a median value of 12 mg/L. The groundwater sample A18 having the highest $SiO_2$ concentration also showed relatively high concentrations of $F^-$ (SM Table 2). Concentrations of B varied from 16 to 380 μg/L and were slightly correlated with $Cl^-$ ($R^2 = 0.488$).

The variation of $NO_3^-/Cl^-$ molar ratios with $Cl^-$ concentrations is an effective tool applied to determine mixing processes and also useful in indicating anthropogenic sources such as sewage leakage and manure and fertilizers (Guo et al., 2020; Nyilitya et al., 2021; Torres-Martinez et al., 2021). Sewage and manure generally are characterized by $NO_3^-/Cl^- < 1$, compared to fertilizers which generally shows $NO_3^-/Cl^- > 10$ (Torres-Martinez et al., 2021). In Fig. 4a,b, $NO_3^-/Cl^-$molar ratios in the sampled groundwaters and two wastewaters were plotted against the $Cl^-$ concentration. All groundwaters sampled from both northern (Fig. 4a) and southern (Fig. 4b) areas showed $NO_3^-/Cl^-$ ratios < 1 indicating a probable dominance of sewage and/or manure as sources of nitrate in the studied areas. Few samples in the southern area (A3, A9, A10, A11; Fig. 4b) showed low $NO_3^-/Cl^-$ ratios and relative low $Cl^-$ concentrations. In Fig. 4c,d sulfate concentration was plotted against the $NO_3^-/Cl^-$ ratio. In Fig. 4d, the samples A3, A9, A10, A11 in the southern area also presented relatively low sulfate concentration, which could suggest possible denitrification in these water samples. Further information may derive from the analysis of temporal variation in nitrate concentrations reported in SM Table 3. In the southern area, samples A3 and A10 showed low nitrate concentrations in 2018, respectively 1.2 and 4.0 mg/L, and in the same order of magnitude respect to the mean concentrations calculated over the 7 years period (1.5 ± 0.5 mg/L and 7.0 ± 1.0 mg/L). Mean nitrate concentrations in sample A9 and A11 were generally high and stable from 2011 to 2017 (respectively 75 ± 14 mg/L and 52 ± 10 mg/L) but showed very low values in 2018 (≤ 1 mg/L). A significant decrease in nitrate concentration (more than the standard deviation calculate over the 2011 to 2017 period) was also observed in 2018 at sampling sites A18, A20 and A58 (SM Table 3).

### 4.3. Isotopic composition of water

Results of deuterium and oxygen-18 isotopes determined in groundwater samples collected in the Northern area and Southern area are reported in SM Table 1 and SM Table 2, respectively.

Fig. 5 shows the relationship between the $\delta^2H$ and $\delta^{18}O$ values in the studied groundwater samples. Most of samples lie close to the GMWL (Global Meteoric Water Line, Craig, 1961) and the IMWL (Italian Meteoric Water Line proposed for southern Italy, Giustini et al., 2016), indicating a meteoric origin of groundwater samples. Groundwater in the Northern area did not undergo significant isotopic fractionation since their infiltration (Fig. 5a). The groundwater A10 in the Southern area showed the less negative values of $\delta^2H$ and $\delta^{18}O$, indicating evaporation; this interpretation is consistent with hydrogeological evidence showing lake water infiltration into this well. The groundwater samples A53 to A62 collected in the Southern area were distinguished by a marked negative $\delta^{18}O$ shift (Fig. 5b), likely indicating oxygen isotopic exchange between the groundwater and the gas phase $CO_2$. These samples were located in correspondence of faults bordering the Campidano Graben (Cocco et al., 2012), where thermal waters occur (Angelone et al., 2005; Frau et al., 2020). Groundwater samples A56 and A58 showed water temperature of 23 and 24 °C, respectively, Na-bicarbonate-chloride composition (SM Fig. 1b), Ca/$HCO_3^-$ molar ratio of 0.14 and 0.19, respectively, and A58 also showed the highest $F^-$ (SM Table 2). These characteristics were similar to the $CO_2$-rich thermal waters of the Campidano, thus explaining the negative $\delta^{18}O$ shift observed in Fig. 5b. However, a potential influence of industrial activities on the $CO_2$ flux in this area cannot be excluded and would need further investigations.

### 4.4. Isotopic composition of sulfate

Results of sulfur-34 and oxygen-18 in $SO_4^{2-}$ determined in groundwater samples collected in the Northern area and Southern area are reported in SM Table 1 and SM Table 2, respectively. Fig. 6 shows values of $\delta^{18}O_{SO4}$ versus $\delta^{34}S$ of $SO_4^{2-}$ in groundwater samples collected in the Northern (a) and Southern (b) areas, together with boxes of potential $SO_4^{2-}$ sources (from Puig et al., 2017). The isotopic compositions indicated different sources of $SO_4^{2-}$ in groundwater samples. Many samples showed isotopic features attributed to $SO_4^{2-}$ derived from the interaction

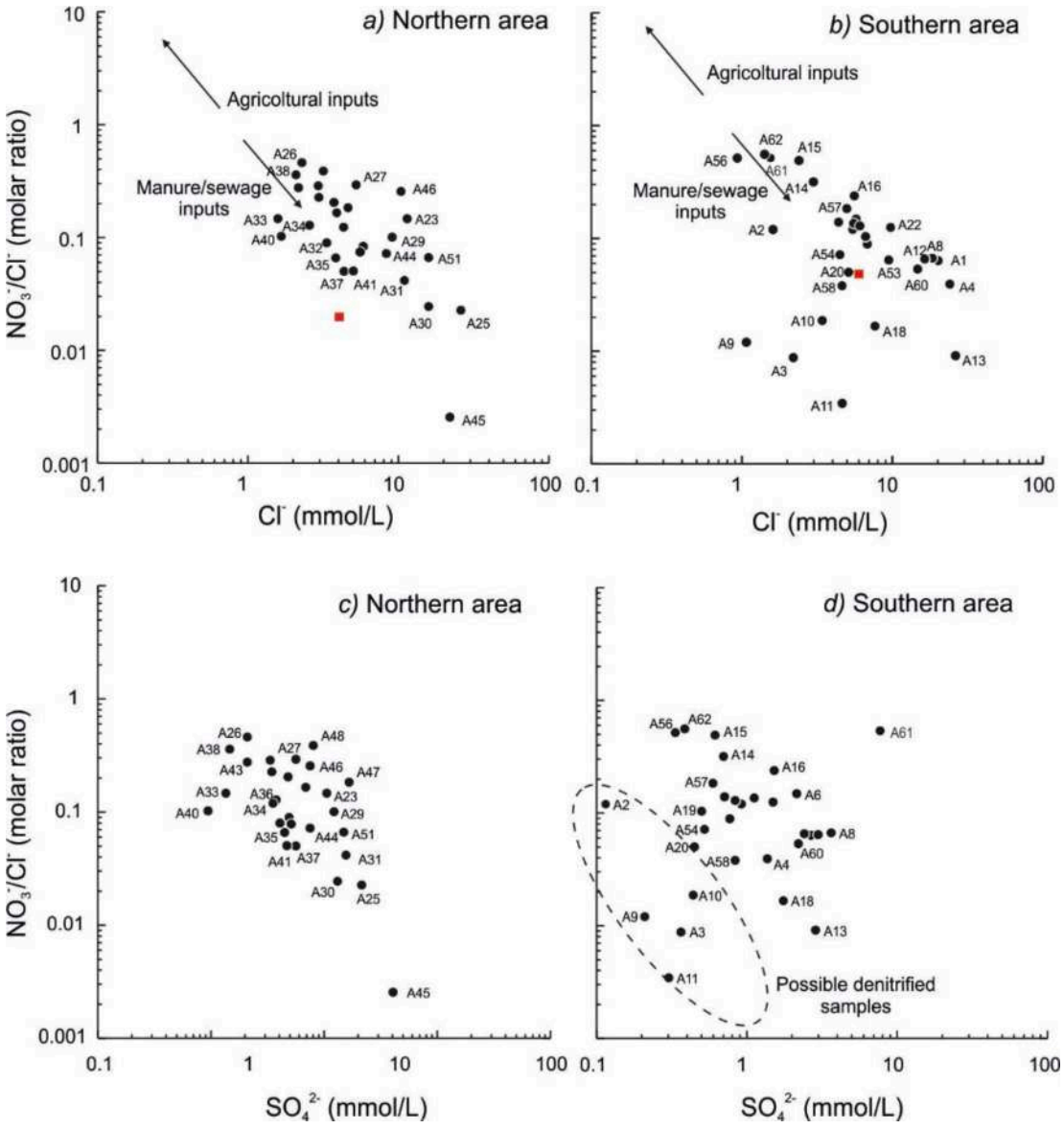


**Fig. 4.** Relationship between the $NO_3^-/Cl^-$ vs $Cl^-$ and $NO_3^-/Cl^-$ vs $SO_4^{2-}$ in groundwater of the Northern area (a, c) and Southern area (b, d). Red symbols in the $NO_3^-/Cl^-$ vs $Cl^-$ plots refer to wastewater samples.

of water with marine sediments. These findings were consistent with the location of these samples in correspondence of marine sediments derived host aquifer. Groundwater samples A38 and A47 (Fig. 6a), and A62 (Fig. 6b) showed $\delta^{18}O_{SO4}$ versus $\delta^{34}S$ values attributed to $SO_4^{2-}$ derived from the oxidation of sulfide minerals. The groundwater sample A61, having a high concentration of $SO_4^{2-}$ (SM Table 2), showed a sulfur isotopic signature attributed to fertilizers (Fig. 6b). Other samples were in the soil, manure, sewage fields, and still others might have isotopic signatures indicating $SO_4^{2-}$ being derived from a mix of different sources.

### 4.5. Nitrate source identification, multi-isotopic approach and SIAR model

Results of nitrogen-15 and oxygen-18 in $NO_3^-$ determined in groundwater samples collected in the Northern area and Southern area are reported in SM Table 1 and SM Table 2, respectively. Fig. 7 shows values of $\delta^{15}N$ and $\delta^{18}O_{NO3}$ of nitrate in groundwater samples collected in the Northern (a) and Southern (b, c) areas.

According to the experimental equation proposed by Andersson and Hooper, 1983, the expected values of $\delta^{18}O_{NO3}$ derived from the nitrification of $NH_4^+$ should range between +3.2‰ and +4.3‰ in the Northern area ($\delta^{18}O_{H2O}$ range: −6.9 to −5.3‰, SM Table 1 and Fig. 7a), from +3.5‰ to +5.3‰ in the Southern area ($\delta^{18}O_{H2O}$ range: −6.5 to −3.8‰, SM Table 2 and Fig. 7b), and from −1.8‰ to +0.8‰ in the group of groundwater that underwent isotopic exchange with $CO_2$ ($\delta^{18}O_{H2O}$ range: −10.5 to −9.0‰,SM Table 2 and Fig. 7c). In Fig. 7a, two groundwater samples in the Northern area showed $\delta^{18}O_{NO3}$ inside the theoretical value of $\delta^{18}O_{NO3}$ derived from nitrification of nitrogen compounds. The source of $NO_3^-$ in sample A45, taking into account the relatively low $NO_3^-$ concentration (3.5 mg/l), below the threshold value (Fig. 3a), could be attributed prevalently to nitrification of $NH_4^+$ contained in the soil. The isotopic values measured in A28 (52 mg/L $NO_3^-$, SM Table 1) could be attributed to nitrification processes at manure/sewage sources, although volatilization of $NH_4^+$ in fertilizers resulting in a $\delta^{15}N$ increase of the residual $NH_4^+$ cannot be excluded (Lasagna and De Luca, 2019; Kendal et al., 2007).

In the Southern area, the groundwater A9 is the only one falling in the field of $NO_3^-$ fertilizers (Fig. 7b). The low concentration of $NO_3^-$ (1 mg/L, SM Table 2) observed at this site appears in contrast with $NO_3^-$ contamination from fertilizers. Results of the RAS monitoring at A9

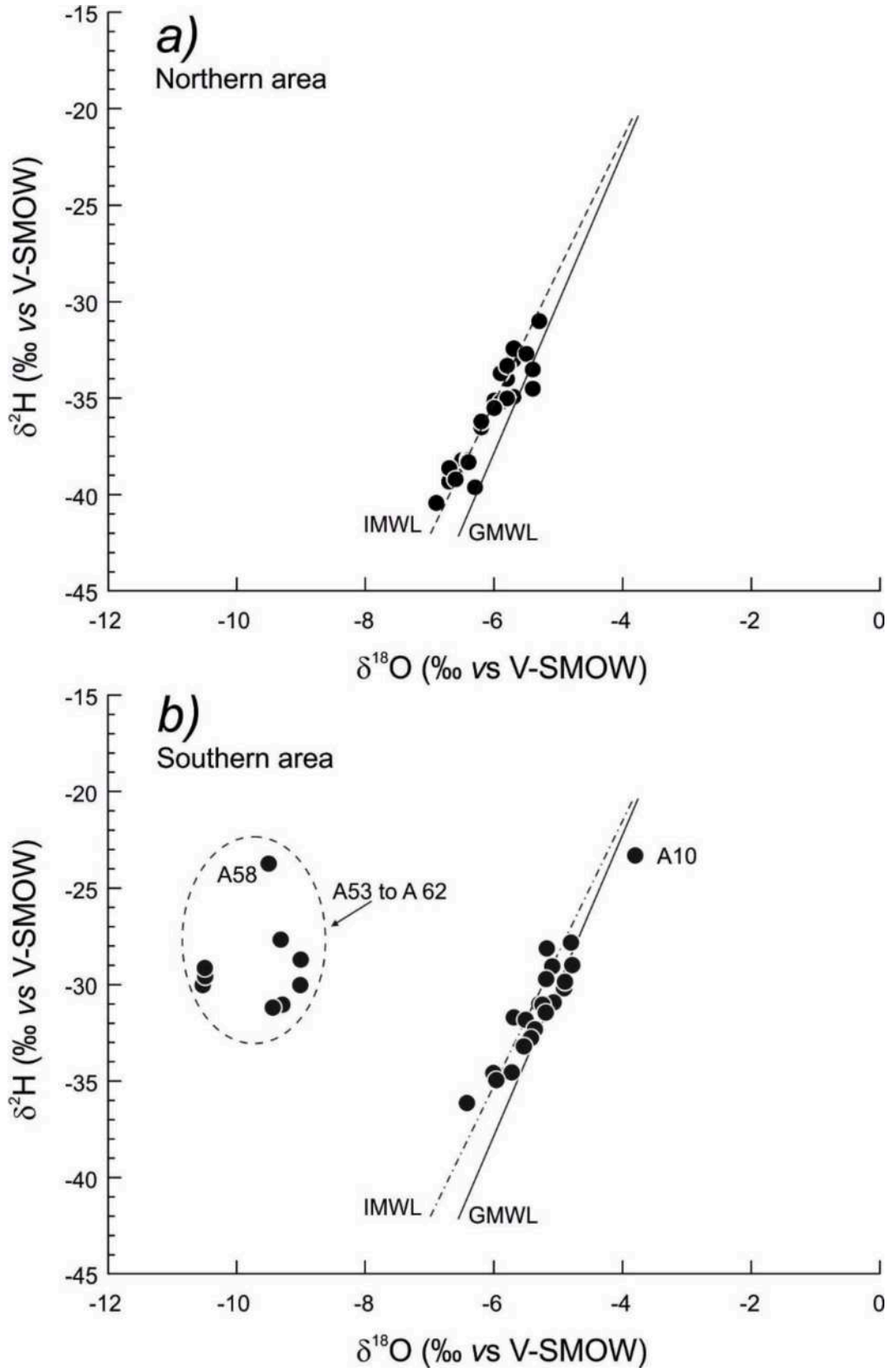


**Fig. 5.** Relationship between the $\delta^2H$ and $\delta^{18}O$ values in groundwater of the Northern (a) and Southern (b) areas. GMWL is the Global Meteoric Water Line (Craig, 1961), IMWL represents the meteoric water line proposed for southern Italy (Giustini et al., 2016). Groundwater samples within the dashed line show a negative $\delta^{18}O$ shift likely indicating oxygen isotopic exchange between groundwater and carbon dioxide.

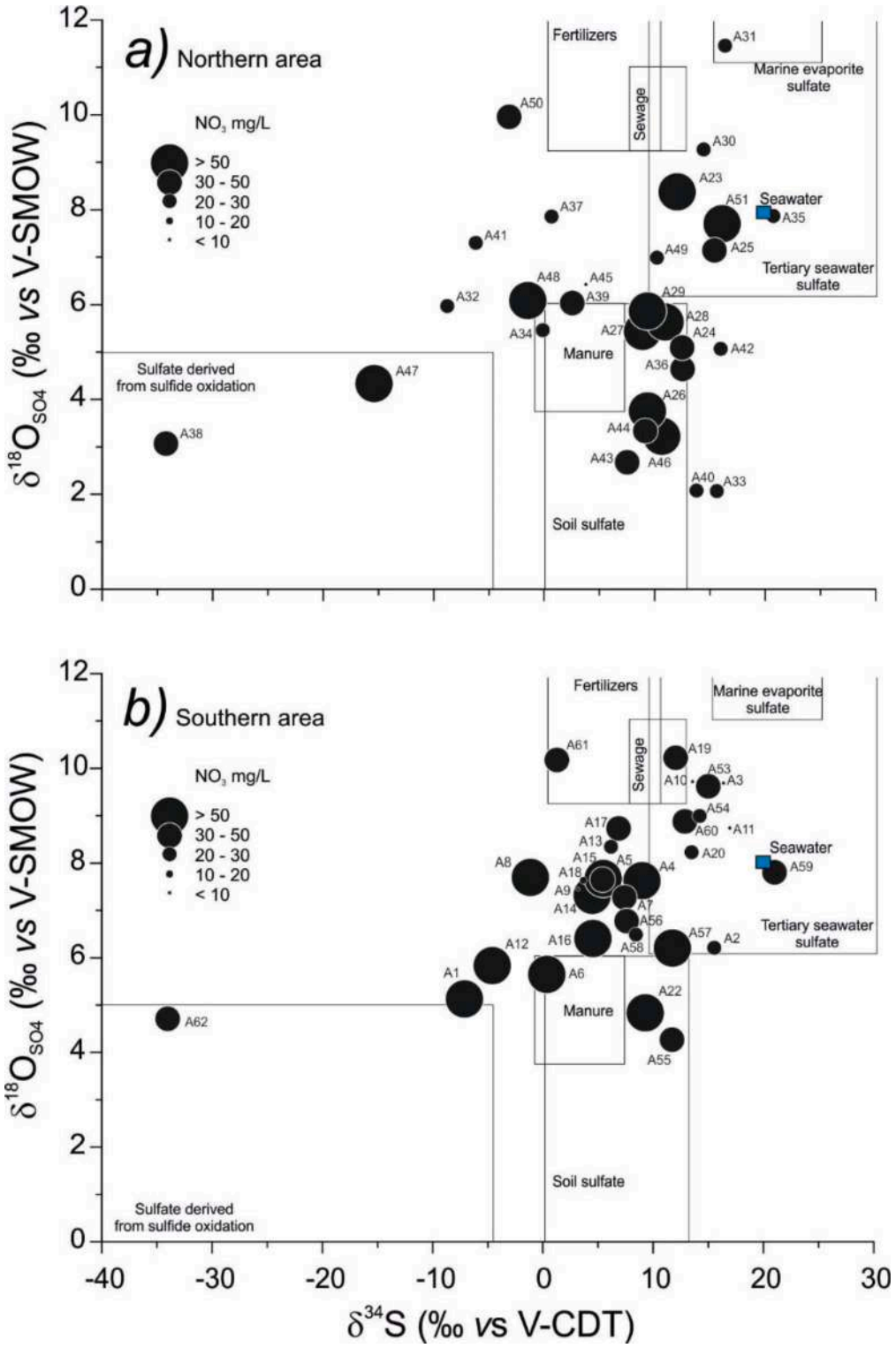


**Fig. 6.** Plot $\delta^{18}O_{SO4}$ versus $\delta^{34}S$ values of sulfate for groundwater samples in the Northern (a) and Southern (b) areas. The boxes show potential sulfate sources derived from Puig et al. (2017).

showed significant temporal variations: high EC and $NO_3^-$ (mean values of 0.98 mS/cm and 75 mg/L, respectively) were observed in the period 2011 to 2017, thereafter EC and $NO_3^-$ decreased (mean values of 0.34 mS/cm and <0.8 mg/L, respectively). Values observed in this study (SM Table 2) suggest dilution by rainwater at the A9 site.

In Fig. 7, some groundwater showed isotopic values of $\delta^{18}O_{NO3}$ higher than the estimated theoretic range for local nitrate $\delta^{18}O$, probably due to the contribution of natural denitrification and/or nitrate from synthetic $NO_3^-$ fertilizer. Denitrification is a microbial mediated process resulting in a natural attenuation of $NO_3^-$ concentration in water systems (e.g.: Kendall et al., 2007). If denitrification occurs, the residual $NO_3^-$ becomes enriched in heavy isotopes, and $\delta^{15}N_{NO3}$ and $\delta^{18}O_{NO3}$ values should follow a positive linear relationship with a $\delta^{18}O_{NO3}/\delta^{15}N_{NO3}$ ratio ranging from 1:1 to 2:1 (Böttcher et al., 1990;

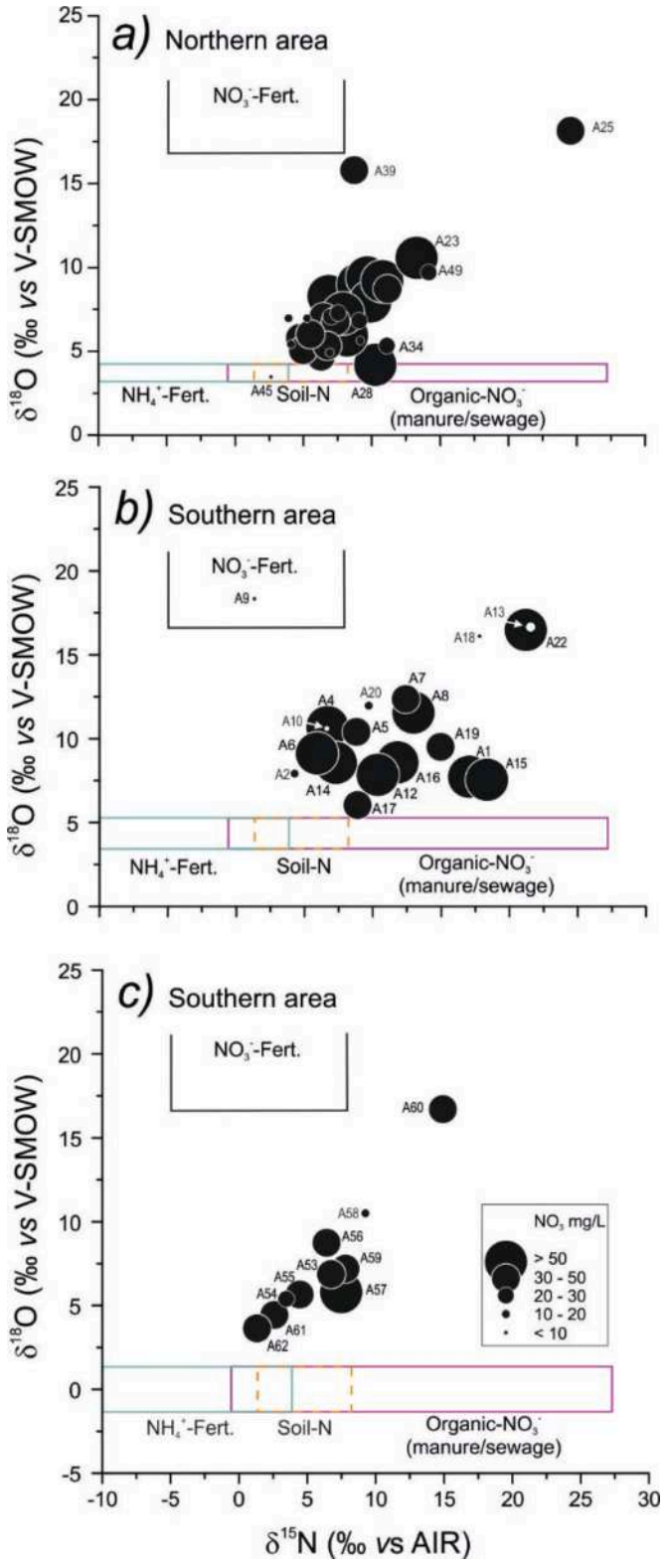


**Fig. 7.** Plot $\delta^{18}O_{NO3}$ versus $\delta^{15}N$ values of nitrate for groundwater samples in the Northern (a) and Southern (b, c) areas. The boxes show potential nitrate sources, with $\delta^{15}N$ values derived from literature (Vitòria et al., 2004; Kendall et al., 2007 and Xue et al., 2009); the local $\delta^{18}O_{NO3}$ values were calculated according to Andersson and Hooper (1983).

Fukada et al., 2003). Trends observed in Fig. 7 indicate that denitrification might have occurred at different degrees. The isotopic compositions of groundwater samples A2, A10, A13, A18, A20 and A58 located in the Southern area coupled with low $NO_3^-$ concentrations in the range of 1.0 to 16 mg/L (SM Table 2) and the relative low sulfate (Fig. 4d) concentration may suggest that denitrification likely affected these groundwater samples in different proportions.

Most samples in southern (A1, A5, A6, A14, A16, A53, A55, A57, A59, A60, A61 and A62) and northern (A21, A23, A24, A25, A26, A27, A29, A30, A33, A36, A38, A39, A40, A42, A43, A44, A48, A51) areas, were characterized by $\delta^{15}N_{NO3}$ and $\delta^{18}O_{NO3}$ enrichment and by relatively high mean concentration of nitrate (mean values in the range of 50 and 240 mg/L, see SM Tables 1, 2 and 3) and a Relative Standard Deviation comparatively low (RSD < 20). It can be inferred that natural denitrification in these samples had probably a moderate impact and/or that $NO_3^-$ attenuation was balanced by the continue input of new $NO_3^-$ into the aquifer.

Because an isotope monitoring and/or experiments for determining enrichment factors of denitrification were not conducted in this study, a rough estimation of the enrichment factor in our systems was derived plotting $\delta^{15}N_{NO3}$ (and $\delta^{18}O_{NO3}$) vs. $\ln(NO_3^-/Cl^-)$ (Li et al., 2019; Kou et al., 2021) with results reported in SM Fig. 2. Significant correlation was not observed in groundwater collected in the Northern area ($R^2 < 0.1$) and for most groundwater collected in the Southern area ($R^2 < 0.1$). An inverse correlation ($R^2 = 0.63$ for $\delta^{18}O_{NO3}$ and 0.67 for $\delta^{15}N_{NO3}$, SM Fig. 2) was observed considering groundwater samples A2, A10, A13, A18, A20 and A58 in the Southern area, however, the estimated enrichment factors (the slope of the regression, ε) seem to suggest a small isotope effect (−5.8 and −2.9 respectively for $\delta^{15}N$ and $\delta^{18}O$). The above observations suggest that the observed variability of $\delta^{15}N$ and $\delta^{18}O$ of nitrate in most samples results prevalently by contributions of different $NO_3^-$ sources in groundwater whereas denitrification seems to play a lesser role. Values of dissolved oxygen (DO) in groundwater range from 2.9 to 9.6 mg/L in the Northern area (SM Table 1) and from 2.0 to 8.9 mg/L in the Southern area (SM Table 2), with average of 6.9 ± 1.7 mg/L and 6.3 ± 1.9 mg/L, respectively. The relationship between $NO_3^-$ and DO in the studied groundwater samples is shown in SM Fig. 3, relatively high concentrations of $NO_3^-$ were associated with either above or below 4 mg/L DO. Concentrations of DO in most of the studied groundwater appeared unsuitable to promote denitrification but it may occur in localized areas of the aquifers (prevalently in the southern area) where favorable conditions may occur in micro-anaerobic parts of the aquifer (Koba et al., 1997; Moncaster et al., 2000; Wu et al., 2018).

The Bayesian mixing model SIAR (Parnell et al., 2010, 2013) has been used to quantify the relative contributions of potential $NO_3^-$ sources in isotopic mixtures (Meghdadi and Javar, 2018; Zhang et al., 2018; Ren et al., 2022). In this paper, two models were run with a different value of the fractionation factors. In model 1 the estimated fractionation factors (see SM Fig. 2) were assumed for the groundwater A2, A10, A13, A18, A20, A58 only, that likely underwent denitrification, and were set to 0 for the other groundwater samples (Jin et al., 2020; Zhang et al., 2020; Kou et al., 2021). Because denitrification seems to play a lesser role but cannot be ruled out, model 2 was run using the estimated fractionation factors (SM Fig. 2) for all samples. Results of the SIAR model are shown in SM Fig. 4a for model 1, and in SM Fig. 4b for model 2. The two models showed evident difference in the proportional contribution of the nitrate sources. However, both models suggested that, in both areas, the highest median contribution of $NO_3^-$ in groundwater was from organic nitrogen derived from sewage and/or manure sources. The second $NO_3^-$ source, i.e. the median contribution of $NO_3^-$ to groundwater from $NH_4^+$ fertilizers, in the Southern area was higher than that observed in the Northern area. The $NO_3^-$ in the groundwater derived from $NO_3^-$ fertilizers and/or the soil occurred in minor proportions in both areas.

While the $\delta^{15}N_{NO3}$ and $\delta^{18}O_{NO3}$ systematic can distinguish several $NO_3^-$ sources, it do not distinguish between manure and sewage derived $NO_3^-$, due to overlapping isotopic signatures. The boron isotope

composition ($\delta^{11}B$) is not affected by biogeochemical transformation processes, such as natural denitrification, therefore, can be used as a conservative tracer (Widory et al., 2004) to identify the impact of wastewaters on the aquatic system and as an indicator of mixing processes. Interaction of water with the aquifer matrix may cause dissolution of B-bearing silicates, adsorption-desorption processes on clays or Fe-hydroxides, thus affecting the isotopic composition and concentration of dissolved B (Xiao et al., 2013).

Results of $\delta^{11}B$ determined in samples collected in the Northern and Southern areas are reported in SM Table 1 and SM Table 2, respectively. Values of $\delta^{11}B$ measured in groundwater showed high variations with similar ranges in the Northern (5.7 ‰ to 43 ‰) and Southern area (5.4 ‰ to 41 ‰), and the same median value (32 ‰). More than 90% of $\delta^{11}B$ values measured in groundwater were higher than +20 ‰, thus in the range reported for manure (7 ‰ to 42 ‰, Widory et al., 2004, 2005; Xiao et al., 2013). The $\delta^{11}B$ values measured in samples collected from wastewater treatment plants varied from 13 ‰ to 25 ‰ with median value of 17 ‰. The values of $\delta^{11}B$ measured in wastewaters collected in the Northern were lower (13‰ to 17‰) than $\delta^{11}B$ measured in wastewaters collected in the Southern area (15‰ to 25‰). The $\delta^{11}B$ values in wastewaters of study areas were generally higher than those reported in literature for sewage (−8 ‰ to 15 ‰, Widory et al., 2005; Xiao et al., 2013). Fig. 8 reports values of $\delta^{11}B$ versus 1/B in groundwater samples, the lowest values of $\delta^{11}B$ were measured in groundwater samples A35 (Fig. 8a) and A15 (Fig. 8b), respectively collected in the Northern and Southern area. The $\delta^{11}B$ values in these samples indicate a source of B derived prevalently from sewage, which is consistent with field evidences. In fact, the sample A35 was collected about 50 m downstream of a wastewater treatment plant and the sample A15 was collected in the urban area of Cagliari, in a well probably affected by leakage of sewage from the sewer network. The sample A37 in the Northern area (Fig. 8a) and samples A4, A7, A8, A10, A17, A18, A20, A58 and A60 in the Southern area (Fig. 8b) are probably affected by discharge of wastewater. In fact, most of these sampling sites were located at (A17, A18, A20) and/or downstream of (A4, A8, A60) urban areas. Natural sources of B may be attributed to the groundwater samples having relatively low concentrations of $NO_3^-$ and B, such as samples A33 and A40 in the Northern area (SM Table 1), and A2, A9, A10 and A11 in the Southern area (SM Table 2). Groundwater sample A51, located close to the coast in the Northern area, showed the highest $\delta^{11}B$ value of 43.0 ‰ (SM Table 1), indeed, a high value in Western Mediterranean environments. Literature values of $\delta^{11}B > 40$ ‰ were observed in saline groundwater in arid/semi-arid regions, such as the Gaza strip (Vengosh et al., 2005), and New Mexico (Langman and Ellis, 2010), and much higher $\delta^{11}B$ values (up to 64 ‰) were determined in brines originated from evaporated seawater in Laizhou Bay, China (He et al., 2018).

Fig. 9 summarizes the spatial distribution of potential $NO_3^-$ sources estimated by the SIAR model and B isotopic signatures in groundwater samples from the Northern (Fig. 9a) and Southern (Fig. 9b) areas. Groundwater samples showing $NO_3^-$ derived from manure and fertilizers were in flat areas where agricultural and farming are more developed. This result is consistent with the use of organic and inorganic fertilizers in cultivated zones in both areas. The higher contribution of $NO_3^-$ from $NO_3$-fertilizers in the Southern area (see Fig. 2b) is also consistent with a larger diffusion of greenhouse crops in the Southern area, where the use of fertilizers is widespread.

## 6. Conclusion

Groundwater in two study areas (Northern and Southern) of Sardinia were investigated to assess $NO_3^-$ contamination prior to the designation of new NVZ. Results of hydrogeochemical and stable isotopes indicate that the groundwater quality in the study areas was affected by both natural processes and anthropogenic activities. The observed geochemical facies, mainly ranging from calcium bicarbonate at low salinity to sodium chloride at increasing salinity, resulted from the interaction of water with the rock-forming minerals of aquifers, and with gas phases, especially $CO_2$. Concentrations of $NO_3^-$ in groundwater occurred in a large range. The present-day background threshold values were 6.6 and 4.3 mg/L $NO_3^-$ in groundwater of the Northern and Southern areas, respectively. Concentrations above $NO_3^-$ threshold in groundwater in both study areas were mostly originated from manure, sewage, and agricultural activities.

Results of the SIAR model showed that the manure & sewage were the predominant sources contributing the highest median value of $NO_3^-$ in groundwater of the study areas, whereas other sources showed minor contributions. Boron isotopic signature showed the manure to be the predominant source of $NO_3^-$ in groundwater.

Nitrification and volatilization processes might have occurred at few sites, and denitrification was likely to occur at specific sites. Geographic areas showing either a predominant process or a specific $NO_3^-$ source were not recognized in groundwater of the studied areas. Mixing among

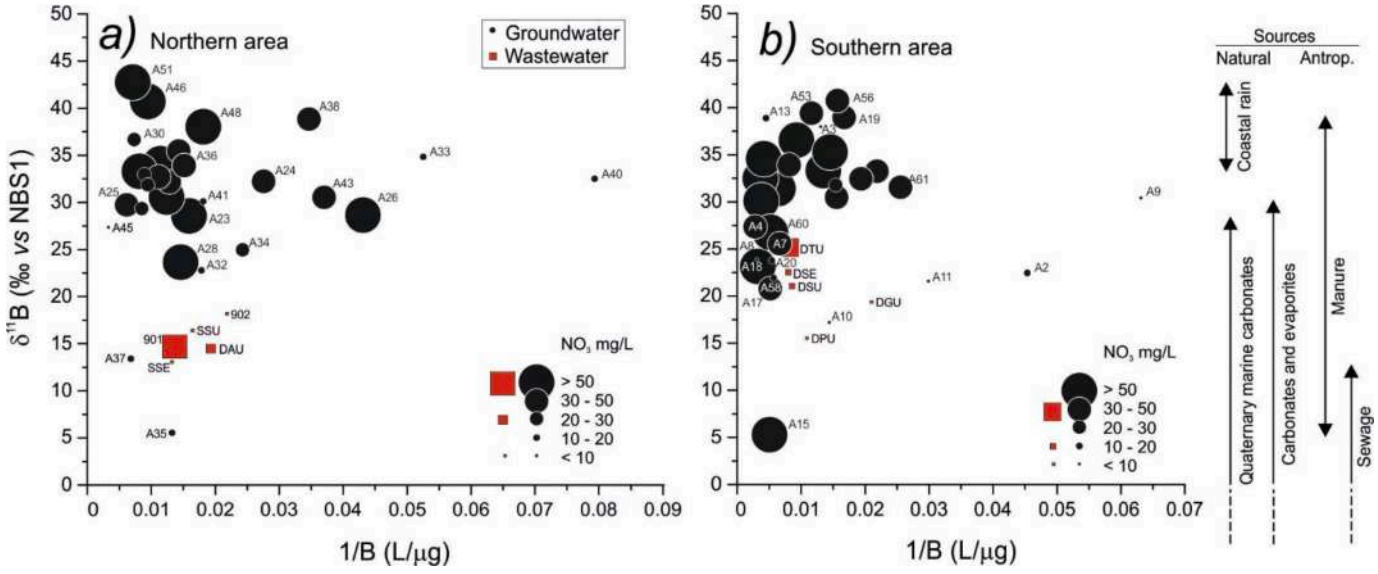


**Fig. 8.** Values of $\delta^{11}B$ versus 1/B for groundwater samples in the Northern (a) and Southern (b) areas, showing potential sources of B in the groundwater and wastewater samples. Ranges of the potential B sources were derived from literature (Widory et al., 2004, 2005; Tirez et al., 2010; Xiao et al., 2013).

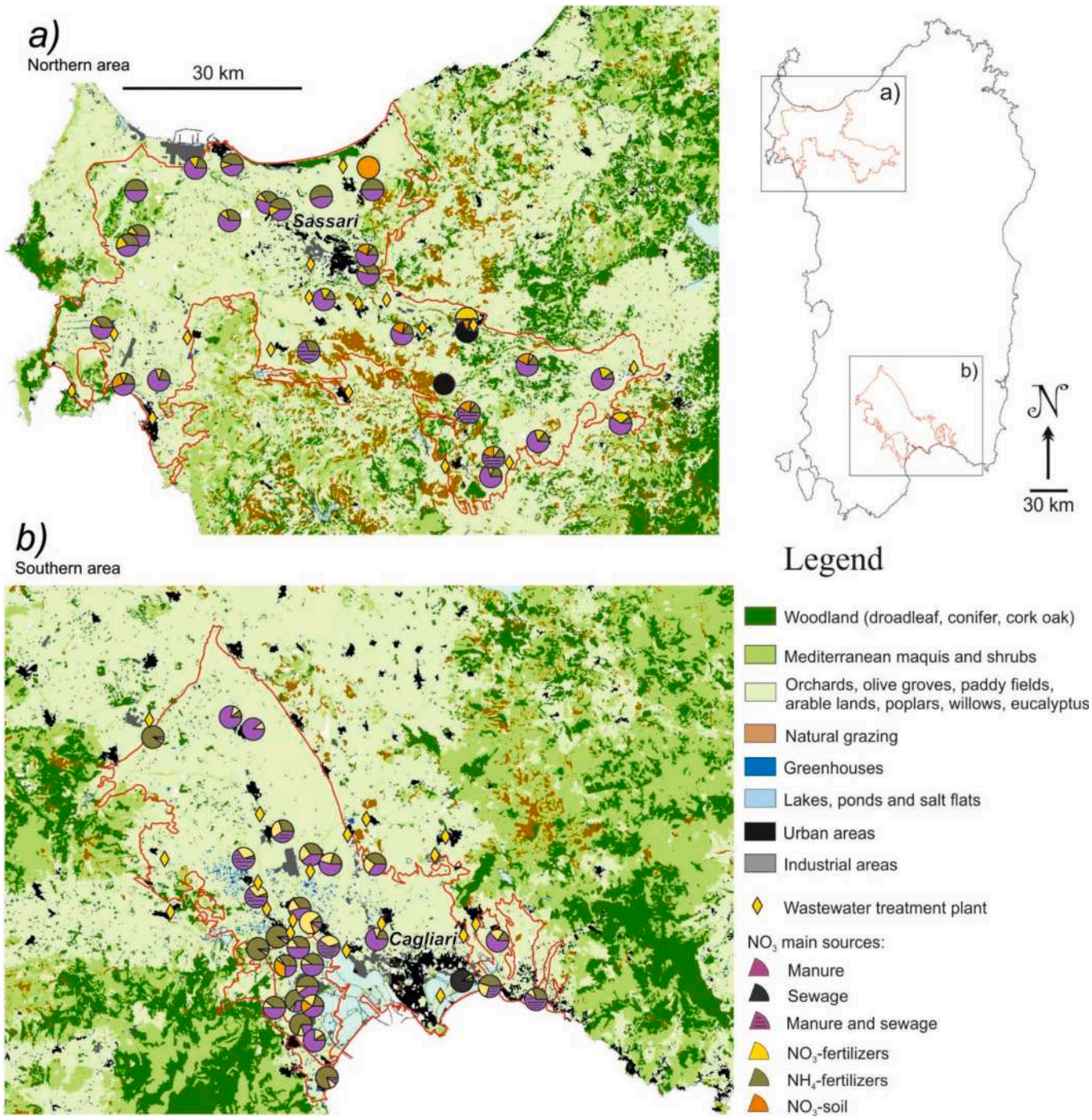


**Fig. 9.** Spatial distribution of the potential $NO_3^-$ sources estimated by isotopic analyses and the SIAR model in groundwater samples from the Northern (a) and Southern (b) areas, together with the simplified soil use map (modified after RAS, 2013b).

various $NO_3^-$ sources in different proportions might account for the measured $NO_3^-$ concentrations and the isotopic compositions of $NO_3^-$ in several groundwater samples of both areas. These findings may be due to point sources of $NO_3^-$ to the aquifers.

Results of the integrated approach applied to two case study in Sardinia (Italy), permits to highlight the strengths of integrating geochemical and statistical methods to provide nitrate source identification as a reference by decision makers to remediate and mitigate nitrate contamination in groundwater. However, as reported in previous studies (Torres-Martinez et al., 2021; Carrey et al., 2021; Re et al., 2021) the results highlighted that, even in the case of well-established methodologies, it is important to take into account the local characteristics to maximize the benefits of the applications of these accurate techniques. Specifically, in the studied areas, the need of further investigations for assessing local sources (e.g. locally used fertilizers) to be used as end-members for the isotopic assessment and mixing modeling for source apportionment, and coupling the chemical monitoring of groundwater with an isotopic monitoring, at least in selected sites, in order to achieve a more systematic understanding of the nitrogen cycling in these areas.

## Declaration of Competing Interest

All authors declare that they have no known competing financial

interests or personal relationships that could have appeared to influence the work reported in this manuscript.

## Data availability

Data will be made available on request.

## Acknowledgements

This work was funded by the Regione Autonoma della Sardegna (STGRI-DSCG Agreement 2016, CIG Z1A2391704,1 Scientific Responsible R. Cidu). Authors thank the Editor and three anonymous Reviewers who contributed to improve the quality of the original manuscript.

## Supplementary materials

Supplementary material associated with this article can be found, in the online version, at doi:10.1016/j.watres.2023.119663.

## References

Andersson, K.K., Hooper, A.B., 1983. $O_2$ and $H_2O$ are each the source of one O in $NO_2^-$ produced from $NH_3$ by Nitrosomonas: 15N-NMR evidence. FEBS Lett. 164 (2), 236–240. https://doi.org/10.1016/0014-5793(83)80292-0.

Angelone, M., Gasparini, C., Guerra, M., Lombardi, S., Pizzino, L., Quattrocchi, F., Sacchi, E., Zuppi, G.M., 2005. Fluid geochemistry of the Sardinian Rift-Campidano Graben (Sardinia, Italy): fault segmentation, seismic quiescence of geochemically 'active' faults, and new constraints for selection of $CO_2$ storage sites. Appl. Geochem. 20, 317–340. https://doi.org/10.1016/j.apgeochem.2004.08.008.

Aravena, R., Mayer, B., 2010. Isotopes and processes in the nitrogen and sulfur cycles. In: Aelion, M.C., Hohener, P., Hunkeler, D., Aravena, R. (Eds.), Environmental Isotopes in Biodegradation and Bioremediation. CRC Press, pp. 201–246.

ARPAS (Agenzia Regionale per la Protezione dell'Ambiente della Sardegna), 2009. Programma d'azione per la zona vulnerabile da nitrati di origine agricola piano di monitoraggio e controllo (attività 2007-2008). Regione Autonoma della Sardegna, Cagliari (in Italian) 45.

Biddau, R., Cidu, R., Da Pelo, S., Carletti, A., Ghiglieri, G., Pittalis, D., 2019. Source and fate of nitrate in contaminated groundwater systems: assessing spatial and temporal variations by hydrogeochemistry and multiple stable isotope tools. Sci. Total Environ. 647, 1121–1136. https://doi.org/10.1016/j.scitotenv.2018.08.007.

Biddau, R., Cidu, R., Ghiglieri, G., Da Pelo, S., Carletti, A., Pittalis, D., 2017. Nitrate occurrence in groundwater hosted in hard-rock aquifers: estimating background values at a regional scale. Italian J. Geosci. 136, 113–124. https://doi.org/10.3301/IJG.2016.03.

Benaglia, T., Chauveau, D., Hunter, D.R., Young, D.S., 2009. Mixtools: an R package for analyzing mixture models. J. Stat. Softw. 32, 1–29. https://doi.org/10.18637/jss.v032.i06.

Böttcher, J., Strebel, O., Voerkelius, S., Schmidt, H.L., 1990. Using isotope fractionation of nitrate–nitrogen and nitrate–oxygen for evaluation of microbial denitrification in sandy aquifer. J. Hydrol. (Amst) 114, 413–424. https://doi.org/10.1016/0022-1694(90)90068-9.

Cao, M., Hu, A., Gad, M., Adyari, B., Qin, D., Zhang, L., Sun, Q., Yu, C.-.P., 2022. Domestic wastewater causes nitrate pollution in an agricultural watershed. Sci. Total Environ. 823, 153680 https://doi.org/10.1016/j.scitotenv.2022.153680.

Carrey, R., Balleste, E., Blanch, A.R., Lucena, F., Pons, P., López, J.M., Rull, M., Solà, J., Micola, N., Fraile, J., Garrido, T., Munné, A., Soler, A., Otero, N., 2021. Combining multi-isotopic and molecular source tracking methods to identify nitrate pollution sources in surface and groundwater. Water Res. 188, 116537 https://doi.org/10.1016/j.watres.2020.116537.

Cocco, F., Funedda, A., Patacca, E., Scandone, P., 2012. Preliminary note on the structural setting of the central-southern Plio-Quaternary Campidano graben (Sardinia). Rendiconti Online Socieà Geologica Italiana 22, 55–57.

Cocco, F., Funedda, A., Patacca, E., Scandone, P., 2013. Plio-Pleistocene extensional tectonics in the Campidano graben (SW Sardinia, Italy): preliminary note. Rendiconti Online Società Geologica Italiana 29, 31–34.

Coplen, T.B., 2011. Guidelines and recommended terms for expression of stable-isotope-ratio and gas-ratio measurement results. Rapid Commun. Mass Spectrom. 25, 2538–2560. https://doi.org/10.1002/rcm.5129.

Craig, H., 1961. Isotopic variations in meteoric waters. Science 133 (3465), 1702–1703. https://doi.org/10.1126/science.133.3465.1702.

Dempster, A.P., Laird, N.M., Rubin, D.B., 1977. Maximum likelihood from incomplete data via the EM algorithm. J. R. Stat. Soc. Series B Stat. Methodol. 39, 1–38. http://www.jstor.org/stable/2984875.

EC (European Commission), 2000. Directive 2000/60/EC of the European Parliament and of the Council of 23 October 2000 establishing a framework for community action in the field of water policy. Off. J. Eur. Communities: Legis. 327.

EC (European Commission), 2006. Council Directive 2006/118/EC, on the protection of groundwater against pollution and deterioration. Off. J. Eur. Commission Brussels.

EEC (European Economic Community), 1991. Council Directive 91/676/EEC of 12 December 1991 concerning the protection of waters against pollution caused by nitrates from agricultural sources. Off. J. Eur. Communities: Legis. 375/1.

ESRI, 2013. Environmental Systems Research Institute. Esri, 380 New York Street, Redlands, California 92373-8100, USA.

Frau, F., Cidu, R., Ghiglieri, G., Caddeo, G.A., 2020. Characterization of low-enthalpy geothermal resources and evaluation of potential contaminants. Rend Lincei Sci. Fis. Nat. 31, 1055–1070. https://doi.org/10.1007/s12210-020-00950-6.

Frontalini, F., Buosi, C., Da Pelo, S., Coccioni, R., Cherchi, A., Bucci, C., 2009. Benthic foraminifera as bio-indicators of trace element pollution in the heavily contaminated santa gilla lagoon (Cagliari, Italy). Mar. Pollut. Bull. 58, 858–877. https://doi.org/10.1016/j.marpolbul.2009.01.015.

Fukada, T., Hiscock, K.M., Dennis, P.F., Grischek, T., 2003. A dual isotope approach to identify denitrification in groundwater at a river-bank infiltration site. Water Res. 37, 3070–3078. https://doi.org/10.1016/S0043-1354(03)00176-3.

Funedda, A., Oggiano, G., Pasci, S., 2000. The Logudoro basin: a key area for the Tertiary tectono-sedimentary evolution of North Sardinia. Boll. Soc. Geol. Ital. 119, 31–38.

Giustini, F., Brilli, M., Patera, A., 2016. Mapping oxygen stable isotopes of precipitation in Italy. J. Hydrol. Reg. Stud. 8, 162–181. https://doi.org/10.1016/j.ejrh.2016.04.001.

Guo, Z., Yan, C., Wang, Z., Xu, F., Yang, F., 2020. Quantitative identification of nitrate sources in a coastal peri-urban watershed using hydrogeochemical indicators and dual isotopes together with the statistical approaches. Chemosphere. https://doi.org/10.1016/j.chemosphere.2019.125364.

He, S., Li, P., Su, F., Wang, D., Ren, X., 2022. Identification and apportionment of shallow groundwater nitrate pollution in Weining Plain, northwest China, using hydrochemical indices, nitrate stable isotopes, and the new Bayesian stable isotope mixing model (MixSIAR). Environ. Pollut. 298, 118852 https://doi.org/10.1016/j.envpol.2022.118852.

He, Z., Ma, C., Zhou, A., Qi, H., Liu, C., Cai, H., Zhu, H., 2018. Using hydrochemical and stable isotopic ($\delta^2H$, $\delta^{18}O$, $\delta^{11}B$, and $\delta^{37}Cl$) data to understand groundwater evolution in an unconsolidated aquifer system in the southern coastal area of Laizhou Bay. China. Appl. Geochem. 90, 129–141. https://doi.org/10.1016/j.apgeochem.2018.01.003.

Jin, Z., Wang, J., Chen, J., Zhang, R., Li, Y., Lu, Y., He, K., 2020. Identifying the sources of nitrate in a small watershed using $\delta^{15}N$-$\delta^{18}O$ isotopes of nitrate in the Kelan Reservoir, Guangxi. China. Agric. Ecosyst. Environ. 297, 106936 https://doi.org/10.1016/j.agee.2020.106936.

Kazakis, N., Matiatos, I., Ntona, M.-.M., Bannenberg, M., Kalaitzidou, K., Kaprara, E., Mitrakas, M., Ioannidou, A., Vargemezis, G., Voudouris, K., 2020. Origin, implications and management strategies for nitrate pollution in surface and ground waters of Anthemountas basin based on a $\delta^{15}N$-$NO_3^-$ and $\delta^{18}O$-$NO_3^-$ isotope approach. Sci. Total Environ. 724, 138211 https://doi.org/10.1016/j.scitotenv.2020.138211.

Kendall, C., Elliott, E.M., Wankel, S.D., 2007. Tracing anthropogenic inputs of nitrogen to ecosystems. Eds. In: Michener, R.H., Lajtha, K. (Eds.), Stable Isotopes in Ecology and Environmental Science, 2nd edition. Blackwell, London, pp. 375–449.

Kim, K.-.H., Yun, S.-.T., Kim, H.-.K., Kim, J.-.W., 2015. Determination of natural backgrounds and thresholds of nitrate in South Korean groundwater using model-based statistical approaches. J. Geochem. Explor. 148, 196–205. https://doi.org/10.1016/j.gexplo.2014.10.001.

Koba, K., Tokuchi, N., Wada, E., Nakajima, T., Iwatsubo, G., 1997. Intermittent denitrification: the application of a $^{15}N$ natural abundance method to a forested ecosystem. Geochim. Cosmochim. Acta 61 (23), 5043–5050. https://doi.org/10.1016/S0016-7037(97)00284-6.

Kou, X., Ding, J., Li, Y., Li, Q., Mao, L., Xu, C., Zheng, Q., Zhuang, S., 2021. Tracing nitrate sources in the groundwater of an intensive agricultural region. Agric. Water Manage. 250, 106826 https://doi.org/10.1016/j.agwat.2021.106826.

Langman, J.B., Ellis, A.S., 2010. A multi-isotope ($\delta_D$, $\delta^{18}O$, $^{87}Sr/^{86}Sr$, and $\delta^{11}B$) approach for identifying saltwater intrusion and resolving groundwater evolution along the Western Caprock Escarpment of the Southern High Plains. New Mexico. Appl. Geochem. 25, 159–174. https://doi.org/10.1016/j.apgeochem.2009.11.004.

Lasagna, M., De Luca, D.A., 2019. Evaluation of sources and fate of nitrates in the western Po plain groundwater (Italy) using nitrogen and boron isotopes. Environ. Sci. Pollut. Res. Int. 26 (3), 2089–2104. https://doi.org/10.1007/s11356-017-0792-6.

Li, C., Li, S.-.L., Yue, F.-.J., Liu, J., Zhong, J., Yan, Z.-.F., Zhang, R.-.C., Wang, Z.-.J., Xu, S., 2019. Identification of sources and transformations of nitrate in the Xijiang River using nitrate isotopes and Bayesian model. Sci. Total Environ. 646, 801–810. https://doi.org/10.1016/j.scitotenv.2018.07.345.

Manu, E., Afrifa, G.Y., Ansah-Narh, T., Sam, F., Loh, Y.S.A., 2022. Estimation of natural background and source identification of nitrate-nitrogen in groundwater in parts of the Bono, Ahafo and Bono East regions of Ghana. Groundw. Sustain. Dev. 16, 100696 https://doi.org/10.1016/j.gsd.2021.100696.

Martinelli, G., Dadomo, A., De Luca, D.A., Mazzola, M., Lasagna, M., Pennisi, M., Pilla, G., Sacchi, E., Saccon, P., 2018. Nitrate sources, accumulation and reduction in groundwater from Northern Italy: insights provided by a nitrate and boron isotopic database. Appl. Geochem. 91, 23–35. https://doi.org/10.1016/j.apgeochem.2018.01.011.

McLachlan, G.J., Peel, D., 2000. Finite Mixture Models. Wiley, New York, p. 419.

Meghdadi, A., Javar, N., 2018. Quantification of spatial and seasonal variations in the proportional contribution of nitrate sources using a multi-isotope approach and Bayesian isotope mixing model. Environ. Pollut. 235, 207–222. https://doi.org/10.1016/j.envpol.2017.12.078.

Menció, A., Mas-Pla, J., Otero, N., Regàs, O., Boy-Roura, M., Puig, R., Bach, J., Domènech, C., Zamorano, M., Brusi, D., Folch, A., 2016. Nitrate pollution of

groundwater; all right…, but nothing else? Sci. Total Environ. 539, 241–251. https://doi.org/10.1016/j.scitotenv.2015.08.151.
Moncaster, S.J., Bottrell, S.H., Tellam, J.H., Lloyd, J.W., Konhauser, K.O., 2000. Migration and attenuation of agrochemical pollutants: insights from isotopic analysis of groundwater sulphate. J. Contam. Hydrol. 43, 147–163. https://doi.org/10.1016/S0169-7722(99)00104-7.
Nyilitya, B., Mureithi, S., Bauters, M., Boeckx, P., 2021. Nitrate source apportionment in the complex Nyando tropical river basin in Kenya. J. Hydrol. (Amst.). https://doi.org/10.1016/j.jhydrol.2020.125926.
Panno, S.V., Kelly, W.R., Martinsek, A.T., Hackley, K.C., 2006. Estimating background and threshold nitrate concentrations using probability graphs. Ground Water 44 (5), 697–709. https://doi.org/10.1111/j.1745-6584.2006.00240.x. PMID: 16961492.
Parnell, A.C., Inger, R., Bearhop, S., Jackson, A.L., 2008. SIAR: stable isotope analysis in R. http://cran.r-project.org/web/packages/siar/index.html.
Parnell, A.C., Inger, R., Bearhop, S., Jackson, A.L., 2010. Source partitioning using stable isotopes: coping with too much variation. PLoS One 5. https://doi.org/10.1371/journal.pone.0009672.
Parnell, A.C., Phillips, D.L., Bearhop, S., Semmens, B.X., Ward, E.J., Moore, J.W., Jackson, A.L., Grey, J., Kelly, D.J., Inger, R., 2013. Bayesian stable isotope mixing models. Environmetrics 24, 387–399. https://doi.org/10.1002/env.2221.
Picetti, R., Deeney, M., Pastorino, S., Miller, M.R., Shah, A., Leon, D.A., Dangour, A.D., Green, R., 2022. Nitrate and nitrite contamination in drinking water and cancer risk: a systematic review with meta-analysis. Environ. Res. 210, 112988 https://doi.org/10.1016/j.envres.2022.112988.
Puig, R., Soler, A., Widory, D., Mas-Pla, J., Domènech, C., Otero, N., 2017. Characterizing sources and natural attenuation of nitrate contamination in the Baix Ter aquifer system (NE Spain) using a multi-isotope approach. Sci. Total Environ. 580, 518–532. https://doi.org/10.1016/j.scitotenv.2016.11.206.
R Development Core Team, 2013. R: A Language and Environment for Statistical Computing. R Foundation for Statistical Computing, Vienna, Austria. http://www.Rproject.org/.
RAS (Regione Autonoma della Sardegna), 2005. Deliberazione Della Giunta Regionale n. 1/12 Del 18/01/2005 Con Cui La Regione Sardegna Ha designato, Quale Zona Vulnerabile Da Nitrati Di Origine Agricola (ZVN), Una Porzione Del Territorio Del Comune di Arborea, Cagliari (in Italian). http://www.regione.sardegna.it/documenti/1_24_20050124153157.pdf (Last accessed in February 2022).
RAS (Regione Autonoma della Sardegna), 2011. Caratterizzazione, Obiettivi e Monitoraggio Dei Corpi Idrici Sotterranei Della Sardegna approvato Con Deliberazione della Giunta Regionale n. 1/16 Del 14/01/2011, Allegato Al Piano di Gestione Del Distretto Idrografico. Regione Autonoma della Sardegna, Cagliari (in Italian). https://www.regione.sardegna.it/documenti/1_328_20130906131252.zip.
RAS (Regione Autonoma della Sardegna), 2013a. Carta Dell'uso Del Suolo in Scala 1: 25.000. http://www.sardegnageoportale.it/argomenti/cartedelsuolo.html (Last accessed in January 2022).
RAS (Regione Autonoma della Sardegna), 2013b. Carta Geologica Di Base Della Sardegna in Scala 1:25000. Regione Autonoma della Sardegna, Cagliari. http://www.sardegnageoportale.it/argomenti/cartageologica.html. Last accessed in January 2022.
Re, V., Kammoun, S., Sacchi, E., Trabelsi, R., Zouari, K., Matiatos, I., Allais, E., Daniele, S., 2021. A critical assessment of widely used techniques for nitrate source apportionment in arid and semi-arid regions. Sci. Total Environ. https://doi.org/10.1016/j.scitotenv.2021.145688.
Ren, K., Pan, X., Yuan, D., Zeng, J., Liang, J., Peng, C., 2022. Nitrate sources and nitrogen dynamics in a karst aquifer with mixed nitrogen inputs (Southwest China): revealed by multiple stable isotopic and hydro-chemical proxies. Water Res. 210, 118000 https://doi.org/10.1016/j.watres.2021.118000.
Ryu, H.-.D., Kim, S.-.J., Baek, U-I., Kim, D-W., Lee, H.-.J., Chung, E.G., Kim, M.-.S., Kim, K., Lee, J.K., 2021. Identifying nitrogen sources in intensive livestock farming watershed with swine excreta treatment facility using dual ammonium ($\delta^{15}N_{NH4}$) and nitrate ($\delta^{15}N_{NO3}$) nitrogen isotope ratios axes. Sci. Total Environ. 779, 146480 https://doi.org/10.1016/j.scitotenv.2021.146480.
Sarkar, S., Mukherjee, A., Duttagupta, S., Bhanja, S.N., Bhattacharya, A., Chakraborty, S., 2021. Vulnerability of groundwater from elevated nitrate pollution across India: insights from spatio-temporal patterns using large-scale monitoring data. J. Contam. Hydrol. 243, 103895 https://doi.org/10.1016/j.jconhyd.2021.103895.
Sinisi, R., Mameli, P., Mongelli, G., Oggiano, G., 2012. Different Mn-ores in a continental arc setting: geochemical and mineralogical evidences from Tertiary deposits of Sardinia (Italy). Ore Geol. Rev. 47, 110–125. https://doi.org/10.1016/j.oregeorev.2012.03.006.
Stumm, W., Morgan, J.J., 1996. Aquatic chemistry, Chemical Equilibria and Rates in Natural Waters. John Wiley & Sons Inc., New York. Third Edition.
Tirez, K., Brusten, W., Widory, D., Petelet, E., Bregnot, A., Xue, D., Boeckx, P., Bronders, J., 2010. Boron isotope ratio (δ11B) measurements in Water Framework Directive monitoring programs: comparison between double focusing sector field ICP and thermal ionization mass spectrometry. J. Anal. At. Spectrom. 25, 964–974. https://doi.org/10.1039/C001840F.
Torres-Martinez, J.A., Mora, A., Mahlknecht, J., Daessle, L.W., Cervantes-Aviles, P.A., Ledesma-Ruiz, R., 2021. Estimation of nitrate pollution sources and transformations in groundwater of an intensive livestock-agricultural area (Comarca Lagunera), combining major ions, stable isotopes and MixSIAR model. Environ. Pollut. 269 https://doi.org/10.1016/j.envpol.2020.115445.
Vengosh, A., Kloppmann, W., Marei, A., Livshitz, Y., Gutierrez, A., Banna, M., Guerrot, C., Pankratov, I., Raanan, H., 2005. Sources of salinity and boron in the Gaza strip: natural contaminant flow in the southern Mediterranean coastal aquifer. Water Resour. Res. 41 (1), W01013. https://doi.org/10.1029/2004WR003344.
Venturi, S., Vaselli, O., Tassi, F., Nisi, B., Pennisi, M., Cabassi, J., Bicocchi, G., Rossato, L., 2015. Geochemical and isotopic evidences for a severe anthropogenic boron contamination: a case study from Castelluccio (Arezzo, central Italy). Appl. Geochem. 63, 146–157. https://doi.org/10.1016/j.apgeochem.2015.08.008.
Vitòria, L., Otero, N., Canals, A., Soler, A., 2004. Fertilizer characterization: isotopic data (N, S, O, C and Sr). Environ. Sci. Technol. 38, 3254–3262.
WHO (World Health Organization), 2011. Nitrate and Nitrite in Drinking Water. Background Document For Development of WHO Guidelines for Drinking Water Quality, p. 31.WHO/SDE/WSH/07.01/16/Rev/1 Geneva.
Widory, D., Kloppmann, W., Laurence Chery, L., Bonnin, J., Houda Rochdi, H., Guinamant, J.-.L., 2004. Nitrate in groundwater: an isotopic multi-tracer approach. J. Contam. Hydrol. 72, 165–188. https://doi.org/10.1016/j.jconhyd.2003.10.010.
Widory, D., Petelet-Giraud, E., Négrel, P., Ladouche, B., 2005. Tracking the sources of nitrates in groundwater using coupled nitrogen and boron isotopes: a synthesis. Environ. Sci. Technol. 39 (2), 539–548. https://doi.org/10.1021/es0493897.
Wu, Y., Xu, L., Wang, S., Wang, Z., Shang, J., Li, X., Zheng, C., 2018. Nitrate attenuation in low-permeability sediments based on isotopic and microbial analyses. Sci. Total Environ. 618, 15–25. https://doi.org/10.1016/j.scitotenv.2017.11.039.
Xiao, J., Xiao, Y.K., Jin, Z.D., He, M.Y., Liu, C.Q., 2013. Boron isotope variations and its geochemical application in nature. Austr. J. Earth Sci. 60 (4), 431–447. https://doi.org/10.1080/08120099.2013.813585.
Xue, D., Botte, J., De Baets, B., Accoe, F., Nestler, A., Taylor, P., Van Cleemput, O., Berglund, M., Boeckx, P., 2009. Present limitations and future prospects of stable isotope methods for nitrate source identification in surface- and groundwater. Water Res. 43, 1159–1170. https://doi.org/10.1016/j.watres.2008.12.048.
Yu, L., Zheng, T., Zheng, X., Hao, Y., Yuan, R., 2020. Nitrate source apportionment in groundwater using Bayesian isotope mixing model based on nitrogen isotope fractionation. Sci. Total Environ. 718, 137242 https://doi.org/10.1016/j.scitotenv.2020.137242.
Zhang, Q., Wang, H., Wang, L., 2018. Tracing nitrate pollution sources and transformations in the over-exploited groundwater region of north China using stable isotopes. J. Contam. Hydrol. 218, 1–9. https://doi.org/10.1016/j.jconhyd.2018.06.001.
Zhang, H., Xu, Y., Cheng, S., Li, Q., Yu, H., 2020. Application of the dual-isotope approach and Bayesian isotope mixing model to identify nitrate in groundwater of a multiple land-use area in Chengdu Plain, China. Sci. Total Environ. 717, 137134 https://doi.org/10.1016/j.scitotenv.2020.137134.
EC (European Commission), 2021. Report from the Commission to the Council and the European Parliament on the implementation of Council Directive 91/676/EEC concerning the protection of waters against pollution caused by nitrates from agricultural sources based on Member State reports for the period 2016–2019. Bruss., 11.10.2021.

## Further reading

McAleer, E.B., Coxon, C.E., Richards, K.G., Jahangir, M.M.R., Grant, J., Mellander, Per. E., 2017. Groundwater nitrate reduction versus dissolved gas production: a tale of two catchments. Sci. Total Environ. 586, 372–389.
Otero, N., Torrentò, C., Soler, A., Menciò, A., Mas-Pla, J., 2009. Monitoring groundwater nitrate attenuation in a regional system coupling hydrogeology with multi-isotopic methods: the case of Plana de Vic (Osona, Spain). Agric. Ecosyst. Environ. 133, 103–113. https://doi.org/10.1016/j.agee.2009.05.007.